Benefits of Dual Propellers for a Coaxial Helicopter

Alexander Stillman PhD Student
Michael McKay PhD Graduate
Farhan Gandhi Redfern Professor, Director
Center for Mobility with Vertical Lift (MOVE)
Rensselaer Polytechnic Institute
Troy, NY, United States

ABSTRACT

A model of a coaxial helicopter with a rigid rotor system is modified to have dual side-mounted propellers. The aircraft is simulated in trim at different flight speeds to investigate the potential benefits of the dual propellers with regard to fault tolerance and yaw control authority. At low speed, the dual propellers impact on the main rotor system actuator failure ranges is analyzed, demonstrating an increase in the allowable trim range from 25-30% in the nominal platform to 50-60% with the dual propeller configuration. Relaxation of the stall constraint for the dual propellers expands the upper rotor maximum actuator limits to the maximum geometric limit, minimum actuator limits for the lower rotor are constrained by the upper rotor stall limits. Upper rotor minimum and lower rotor maximum actuator limits are determined by tip clearance restrictions. At mid speed, the dual propellers improve the yaw control power in the 50-100 kt range and allow for a Level 1 aggressive yaw response as defined in ADS-33E. At high speed, the dual propellers provide yaw control redundancy and allow for trim when the rudder is fully deflected for nearly the entire flight envelope.

INTRODUCTION

Coaxial helicopters have solidified their place in modern vertical lift with concept vehicles, like S-97 RAIDER® and SB>1 DEFIANT®, progressing through flight testing and being considered for adoption into service through the Army's Future Vertical Lift Program (Ref. 1). Modern coaxial helicopters use a variety of advanced methods and technologies to push boundaries in helicopter capability. The utilization of rigid, counter-rotating rotors provides high control authority and an expanded flight envelope by alleviating retreating blade stall, allowing for a marriage of traditional helicopter capabilities and future high speed mission requirements. Modern fly-by-wire control architectures allow for advanced control augmentation, further improving the handling qualities and performance of these future vehicles, and allowing for specialized control laws to be used in different flight conditions.

The most common coaxial platform is a coaxial-pusher, featuring a pusher propeller instead of a tail rotor. This design has been thoroughly explored with respect to trim performance (Refs. 2–4), steady and dynamic loads (Refs. 5, 6), and flight control and handling qualities (Refs. 7–10). This work has pointed out unique benefits and drawbacks of the configuration. Recently at RPI, studies have been performed considering the available redundant controls on the coaxial-pusher configuration. Part of this work (Ref. 11) focused on using these redundant controls to trim the aircraft in hover and forward flight in the event of a swashplate actuator locked failure, finding that the coaxial-pusher configuration is capable of re-trimming with different conditions of swashplate actuator failure, however tip clearance limitations constrain certain trim cases. Further work done in collaboration with the US Army extended from trim analysis in the flight control and dynamic simulation (Ref. 12). More details from this project are given in Ref. 13.

A major issue that the was observed in the fault tolerance studies was a lack of yaw authority from the main rotor system. McKay et. al (Ref. 12) shows this issue is most relevant in the case of rudder failure in forward flight. Typically on a coaxial helicopter, yaw control in hover and low speed is achieved using differential collective and in high speed forward flight is achieved using the rudder. In the case of rudder failure in forward flight, rotor controls (differential collective and cyclic inputs) will need to be used to balance the aircraft in yaw. These controls are known to result in degradation of tip clearance (Refs. 11–13). Both the RPI Coaxial Helicopter Analysis and Dynamics code (CHAD, Ref. 13) and the US Army generic coaxial helicopter model (Ref. 8) show that as flight speed increases, yaw control capability from the differential collective is reduced. The result is a yaw control issue where at mid speed, there is inadequate yaw control for the aircraft due to reduced differential collective authority and lack of dynamic pressure for the rudder, and at high speed there is no redundancy for yaw control in the case of rudder failure.

Potential solutions to the yaw control authority issue have been presented in the past, among these is the use of monocyclic on the pusher propeller (Ref. 8). This is shown to create some level of redundancy for yaw in mid to high speed flight, but does not substantially increase the overall yaw control power for the vehicle in the mid speed range of interest. Another potential solution is to change the aircraft configu-

Presented at the Vertical Flight Society's 78th Annual Forum & Technology Display, Ft. Worth, Texas, USA, May 10–12, 2022.

ration and introduce a solution using dual, laterally mounted propellers. This type of aircraft configuration exists on the Airbus RACER (Refs. 14, 15) and X^3 (Ref. 16) compound helicopters, dual propulsors were also present on the XH-59A coaxial helicopter (Ref. 17). Further, academic research efforts have considered use of dual propellers, even within the context of fault tolerance, on a compound helicopter model (Ref. 18). Also investigated are the additional benefits of the dual propellers in low speed flight, as the redundant control allows for increased swashplate actuator failure range.

MODEL DETAILS

RPI's Coaxial Helicopter Analysis and Dynamics (CHAD) code is used for the trim analyses (Ref. 13). CHAD utilizes a blade element theory model coupled with a pressure potential superposition inflow model (PPSIM, Ref. 19) to calculate rotor forces and moments for a given operating condition and control input. This rotor model has been presented and validated in prior publication by the authors (Ref. 11) against coaxial rotor test data from NACA (Ref. 20) and UT Austin (Ref. 21). The aircraft fuselage and control surfaces are modeled using look up tables based on the published XV-15 simulation model (Ref. 22), with appropriate scaling to represent the X2 Technology™ Demonstrator (X2TD). The pusher propellers are modeled with blade element vortex theory (Ref. 23). The CHAD bare-airframe model has a total of 50 states: 12 rigid body, 32 rotor (2 blade modes × 4 blades × 2 rotors × 2), and 6 main rotor inflow (3 states per rotor). CHAD predictions have previously been validated against static rotor performance, vehicle trim performance, and bare-airframe dynamic responses in previous publication by the authors. A full model description and presentation of the full set of validation results can be found in Ref. 13, and will not be presented herein.

Rotor Controls and Swashplate Representation

The rotor controls as defined in this study represent the inputs to the rotor head with a constant 37.5° control phase angle (Γ) that is seen to absorb the phase lag associated with rotor blade dynamics and aerodynamic interference effects. For a typical rotor, there are 3 independent controls traditionally represented by a collective pitch as well as two cyclic inputs. In most helicopter control systems, these controls define the blade pitch at any point about the azimuth as

$$\theta(\psi) = \theta_0 + \theta_{1c}cos(\psi+\Gamma) + \theta_{1s}sin(\psi+\Gamma) \tag{1}$$

where θ_0 is the collective and θ_{1c} and θ_{1s} are the once per revolution cosine and sine cyclic pitch inputs to the rotor, respectively. With two rotors present on a coaxial helicopter, there are 6 independent controls, which can be represented as 3 unique controls to each rotor or a combination of controls. For this study, the rotor controls are defined as follows in Table 1.

Table 1. Coaxial Rotor Controls

Control	Description
θ_0	Symmetric Collective
θ_{lon}	Symmetric Longitudinal
θ_{lat}	Symmetric Lateral
$\Delta\theta_0$	Differential Collective
$\Delta\theta_{lon}$	Differential Longitudinal
$\Delta\theta_{lat}$	Differential Lateral

Using these controls, the individual rotor pitch can be described using Eqs. 2 and 3.

$$\begin{aligned}\theta_U(\psi_U) = (\theta_0+\Delta\theta_0) + (\theta_{lon}+\Delta\theta_{lon})cos(\psi_U+\Gamma)\\ +(\theta_{lat}+\Delta\theta_{lat})sin(\psi_U+\Gamma)\end{aligned} \tag{2}$$

$$\begin{aligned}\theta_L(\psi_L) = (\theta_0-\Delta\theta_0) + (\theta_{lon}-\Delta\theta_{lon})cos(\psi_L+\Gamma)\\ -(\theta_{lat}-\Delta\theta_{lat})sin(\psi_L+\Gamma)\end{aligned} \tag{3}$$

The rotor head control naming convention is opposite to standard convention, where the lateral and longitudinal cyclic inputs are named from the predominant flap response, and therefore are the cosine and sine component of the cyclic pitch input, respectively. With this coaxial model, due to the large stiffness of the rotor, the cosine and sine components of the cyclic inputs result in dominant on-axis flap responses, and so are named longitudinal and lateral for the present study.

Another key component in the rotor controls is the swashplate actuator geometry. To this end, a generic swashplate geometry is developed to analyze different flight conditions and potential limiting situations for the rotor system. The derivation is straightforward, requiring the minimum and maximum collective pitch allowable at the rotor head as well as the azimuthal positions of the swashplate servo actuators on the non-rotating swash plate.

First, consider the normalized throw of a servo actuator, that is $s \in [0,1]$. Note that if all actuators are in the minimum position, the blade pitch will, by definition, exist at the minimum allowable collective setting. It follows similarly for the maximum servo position and maximum collective setting. Defining this allowable collective range as $\theta_0 \in [\theta_{min}, \theta_{max}]$, at the azimuthal position of the i^{th} servo, the blade root pitch is

$$\theta(\psi_i) = (\theta_{max}-\theta_{min})s + \theta_{min} \tag{4}$$

Equating the above expression and Eq. 1 for the local blade root pitch gives the mapping from actuator to rotor head controls as

$$T_{\theta/s}\begin{bmatrix}s_1\\s_2\\s_3\end{bmatrix} + b_{\theta/s} = T_\theta\begin{bmatrix}\theta_0\\\theta_{1c}\\\theta_{1s}\end{bmatrix} \tag{5}$$

$$T_{\theta/s} = (\theta_{max}-\theta_{min})\begin{bmatrix}1&0&0\\0&1&0\\0&0&1\end{bmatrix} \tag{6}$$

$$b_{\theta/s} = \begin{bmatrix} \theta_{min} & \theta_{min} & \theta_{min} \end{bmatrix}^T \tag{7}$$

$$T_\theta = \begin{bmatrix} 1 & \cos(\psi_1 + \Gamma) & \sin(\psi_1 + \Gamma) \\ 1 & \cos(\psi_2 + \Gamma) & \sin(\psi_2 + \Gamma) \\ 1 & \cos(\psi_3 + \Gamma) & \sin(\psi_3 + \Gamma) \end{bmatrix} \tag{8}$$

Note that this is a generalized and simple representation of a swashplate. In reality swashplate geometry is more complex with other limitations defining the relationship between actuator position and rotor head controls. This relation, however, allows for extraction of the general relation between actuators (in certain positions) and rotor head controls, which can assist in identifying flight conditions where actuators may be at relatively extreme positions. The ability to translate pitch control to actuator position can also allow for the identification of ranges of positions that exist throughout large portions of the flight envelope, which can imply aircraft trim for a locked swashplate actuator.

For the present study, the swashplate actuators are assumed to be located at 0°, 180°, and 270° in the appropriate swashplate azimuthal coordinates. The results that follow assume an allowable collective setting range from -5 to 15 degrees on each rotor, which results in a $\pm 10°$ range in θ_{1c} and $\pm 20°$ in θ_{1s} according to the defined model.

PAPER OVERVIEW AND APPROACH

In this study, the tail mounted propeller (Fig. 1) is removed and replaced with two side mounted propellers (Fig. 2). The propeller dimensions, lateral offset, and operating parameters are listed in Table 2. The propellers are aligned with the CG along the waterline and fuselage station lines (vertically and longitudinally), with an offset in the buttline (lateral) position to allow for yaw authority.

Table 2. Propeller Specifications

Property	Value
CG Offset	3 m
Rotor Radius	0.75 m
Propeller Speed	3500 RPM
Number of Blades	6

The propeller controls consist of a collective input to both props for net thrust and a differential input to result in a yaw moment. The collective and differential inputs define the total input for propeller i as shown in Eq. 9

$$\theta_{prop,i} = \frac{\theta_{0,prop} - \Delta\theta_{0,prop} * (-1)^i}{2} \tag{9}$$

where $\theta_{prop,i}$ is the pitch input for propeller i, $\theta_{0,prop}$ is the collective pitch input to the propellers, and $\Delta\theta_{0,prop}$ is the differential propeller pitch input to the propellers.

Nominal trim for this aircraft is defined in Table 3.

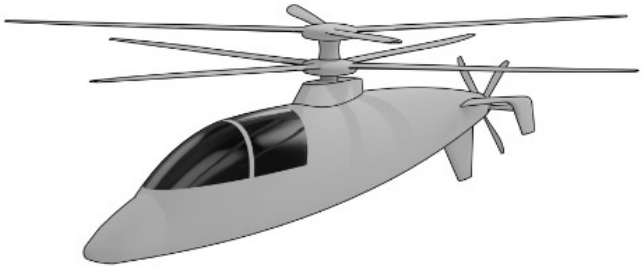

Figure 1. Standard Single Pusher Propeller Coaxial Helicopter

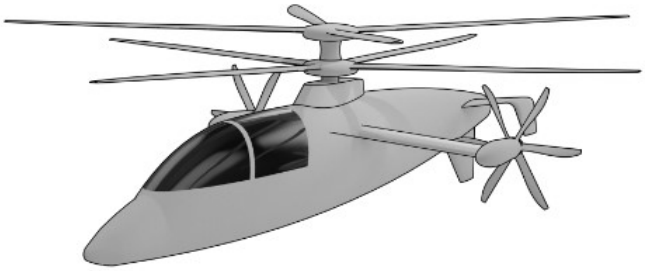

Figure 2. Coaxial Helicopter with Side Mounted Propellers

Table 3. Nominal Trim Setup

Condition	Trim Target	Trim Variable
0 Lon. Accel.	$\dot{u}_b = 0$	$\theta_{0,prop}$
0 Lat. Accel.	$\dot{v}_b = 0$	ϕ_b
0 Vert. Accel.	$\dot{w}_b = 0$	θ_0
0 Roll Accel.	$\dot{p}_b = 0$	θ_{lat}
0 Pitch. Accel.	$\dot{q}_b = 0$	θ_{lon}
0 Yaw. Accel.	$\dot{r}_b = 0$	$\Delta\theta_0$ or δ_r
Lift Offset	LOS Target	$\Delta\theta_{lat}$
Diff Pitch Moment	$\Delta M_{mr} = 0$	$\Delta\theta_{lon}$
Pitch Attitude	θ_b Schedule	θ_b
Yaw Control	Use $\Delta\theta_0$ OR δ_r	$\Delta\theta_0$ or δ_r
Diff Prop	$\Delta\theta_{0,prop} = 0$	$\Delta\theta_{0,prop}$
Tot Pitch Moment	$M_{mr} = 0$	δ_e

To summarize the table briefly, nominal trim requires that vehicle accelerations in the six degrees of freedom be zero, which is achieved by use of the collective propeller feathering, aircraft roll attitude, coaxial symmetric controls, and differential collective below 60 kts or rudder above 60 kts. Further, differential cyclic controls are used to drive the rotor to lift offset schedules for differential roll and pitch moments at the rotor, the vehicle pitch attitude is scheduled to be nose up at 2.75° above 120 kts, differential propeller feathering is not used in trim, and the elevator pitch is set to reduce the total rotor pitching moment.

RESULTS

The results presented in the present work cover three speed ranges, defined as low (0-60 kts), mid (50-100 kts), and high speed (>100 kts). At each condition, the impact of the dual propeller configuration will be laid out in terms of benefit to the air vehicle performance.

LOW SPEED ANALYSIS

The low speed trim analysis is focused on using the dual propellers to increase the trimmable actuator failure ranges. At low speed, the propellers function as a redundant yaw control which can be used to compensate for off-nominal conditions brought about by swashplate actuator failure. Previously (Ref. 11), analysis indicated that at low speed (20 kts) the only option for vehicle trim with swashplate actuator failure is use of large differential cyclic inputs to allow for one rotor to compensate for the undesired loads produced by the rotor with failed actuator. This necessarily changed the tip clearance of the coaxial rotor system, and therefore had fairly restrictive range of allowable locked settings. With the addition of another effector in the yaw axis, the rotors no longer are required to torque balance in the event of swashplate actuator failure, and so a differential collective input can be utilized to expand the allowable ranges for potential failure relative to the traditional coaxial-pusher configuration. A similar approach is taken as was in Ref. 11, where the lift offset of the rotor system is varied in order to explore actuator trim ranges, but now with the ability to compensate for a net torque from the dual rotors, an additional sweep of differential collective is included to potentially expand the tolerable fault range of the actuators.

Lift Offset and Differential Propeller Sweep

With the two rotors present on a coaxial helicopter, forces and moments generated on one rotor can be countered with the other, something that can be achieved by use of differential cyclic pitch. The moments generated by the differential lateral and longitudinal controls do not result in rigid body accelerations, but apply bending loads and tilt the rotor planes towards each other, resulting in a reduction in tip clearance. The differential cyclic controls expand the failure range of the main rotor actuators (as illustrated in Ref. 11). Additionally, use of differential collective pitch can expand the actuator failure ranges, however a net yaw moment is generated that must be compensated in some way. The dual propellers introduce a new yaw control mechanism that can counter the torque from differential collective.

To explore the range of allowable actuator settings, the lateral and longitudinal lift offsets of the rotor system are varied $\pm 20\%$ from nominal trim and the differential propeller pitch is varied $\pm 30^\circ$ in a three dimensional sweep. Past this differential propeller setting, one or both of the propellers stall, precluding a larger yaw moment and not allowing for trim beyond this point. Figure 3 gives the actuator ranges for each of the six main rotor actuators. The solid lines indicate the actuator failure ranges without the differential propellers, using only the lift offset sweep (consistent with Ref. 11). These ranges are restricted by the 11 inch tip clearance limit due to the differential flap response of the two rotors, allowing for somewhere between 25-30% of the overall actuator range to be trimmed at a given flight speed.

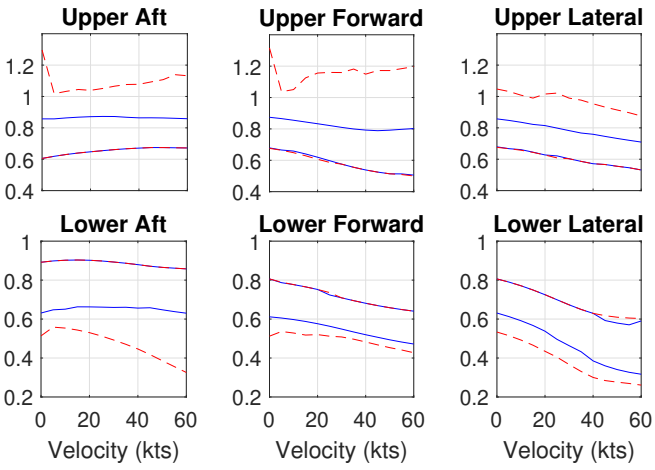

Figure 3. Actuator Failure Ranges

The dashed lines on Fig. 3 indicate the actuator failure ranges with use of the differential thrust from the propellers. The outer actuator failure ranges (upper rotor actuator maximums and lower rotor actuator minimums) are increased from the case without dual propellers due to the use of differential collective. All the actuators of the upper rotor are moved upwards while the lower rotor actuators are moved downwards. This is combined with the lift offset sweeps introducing cyclic controls to achieve the maximum upper actuator and minimum lower actuator trimmable limits.

The inner failure ranges of the actuators (upper rotor minimums and lower rotor maximums) are limited by tip clearance. These limits are more consistent with previous results not using dual propellers in low speed due to the same observed tip clearance limit (Ref. 11). It should be noted, however, that the results in Fig. 3 using the dual propellers represent an expanded range of allowable actuator settings in the low speed range presented.

Without the dual propellers, allowable ranges are observed to be approximately 25-30% of the total actuator throw, with the dual propellers that range expands to upwards of 50-60% of the actuator throw in hover (for specific actuators) and larger expansions at increased speeds. Overall, the addition of the dual propellers expands the trimmable range of all six actuators over the entire range of speeds considered here. Note that some cases indicate allowable upper limits greater than 1, indicating that it would be tolerable to fail these actuators at or even above their assumed maximum limit.

LOS and Diff Propeller Sweep, Unlimited Propeller Thrust

A second trim sweep is performed without constraints on the propeller thrust, representing a re-design of the propellers (increase in RPM, radius, etc.) where stall no longer becomes a limit case as it is in Fig. 3. This sweep finds the restrictions from the main rotors instead of limiting the actuator ranges due to the capability of the hypothetical propellers. Specifically, expansion of the upper actuator maximum failure limits and lower actuator minimum failure limits are explored as they were previously determined by propeller stall.

The actuator failure ranges from the unlimited propeller thrust case are compared to the standard configuration and limited propeller cases in Fig. 4. Actuator limits with unconstrained propeller thrust are shown with the dot-dashed lines, outer limits from Fig. 3 are shown with the dashed lines, and the actuator outer limits of the standard configuration are shown with the solid lines.

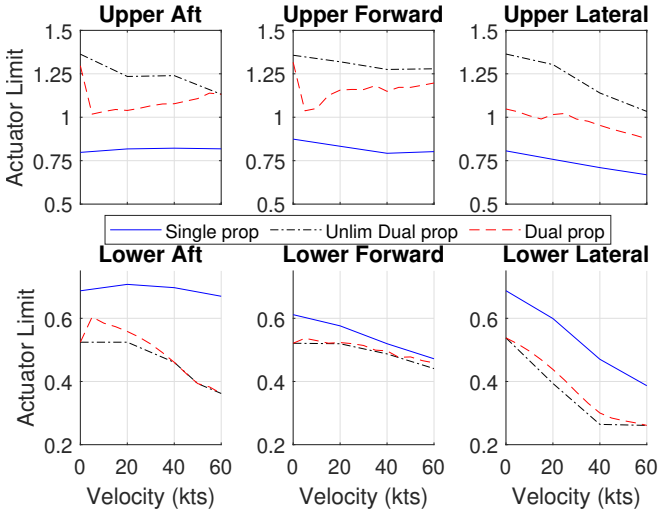

Figure 4. Actuator Limits with Unlimited Propeller Thrust

The upper rotor actuator limits are increased to the point that all the upper rotor actuators can fail at their maximums at all speeds, though this limit decreases towards the limited propeller case as the flight speed increases. The lower rotor actuators do not see the same level of expansion as the upper actuators due to the thrust distribution between the upper and lower rotors. In order to push the lower rotor actuators down, the upper rotor must generate more thrust (i.e. increase average actuator position and, therefore, collective pitch). Due to stall, there is a limit to the thrust that the upper rotor can produce, so the lower actuators cannot be dropped significantly further without creating a thrust imbalance. Further, as the upper rotor becomes more and more heavily loaded (produces more and more thrust), the induced downwash from the rotor increases which then propagates to the lower rotor, engulfing it in a strong field of downwash. In addition to the upper rotor approaching stall, this leads to the lower rotor generating less thrust, and in extreme conditions near the limit cases presented in Fig. 4 the lower rotor can actually produce a download, further increasing the requirements of the upper rotor.

A sweep of collective pitch for the upper rotor identifies the stall limit at 25 degrees, as seen in Fig. 5. Further consideration of the trim conditions defined along the upper rotor maximum or lower rotor minimum limits indicates the collective pitch input plus the differential collective input puts the upper rotor close to stall. Additionally, when cyclic controls are added to achieve the desired lateral and longitudinal lift offset, a portion of the upper rotor is driven to a higher blade pitch and stalls, preventing the upper rotor from generating enough thrust. However, the relaxation of propeller stall limitations is still observed to further expand the allowable trim actuator ranges for the coaxial rotor system, typically expanding the allowable range by 10% or more relative to the stall limited case.

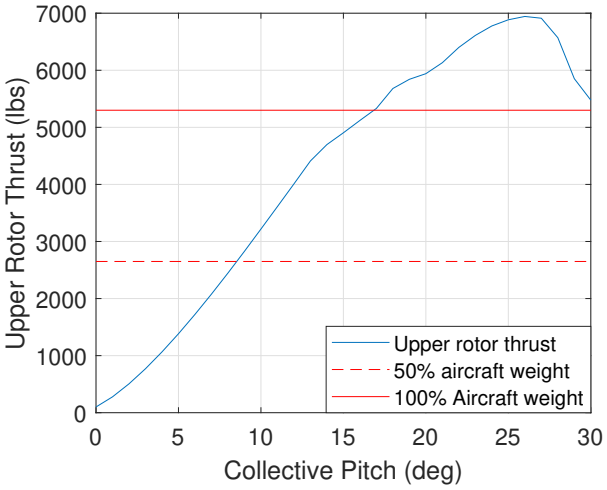

Figure 5. Upper Rotor Thrust vs. Collective Pitch

MID SPEED

The investigation at mid speed centers around the yaw control authority of the aircraft, comparing the standard yaw controls to the dual propellers. The yaw control sensitivity of the different controls, which are obtained via a linearized model of the aircraft dynamics, are compared to one another versus flight speed in Fig. 6.

At low speed, differential collective ($\Delta\theta_0$) is the most sensitive yaw control. As the flight speed increases, its sensitivity falls off until it is no longer effective due to a growing relative upwash through the rotors with flight speed. This sensitivity approaches zero at 100 kts, and is not used above that speed. At the same time, the differential longitudinal cyclic control ($\Delta\theta_{lon}$) and the rudder (δ_{rudder}) yaw sensitivity increase with flight speed. For the rudder, effectiveness increases quadratically as the dynamic pressure increases, which is expected. Differential longitudinal cyclic creates a yaw moment by tilting the rotor tip path planes in opposite directions, tilting the

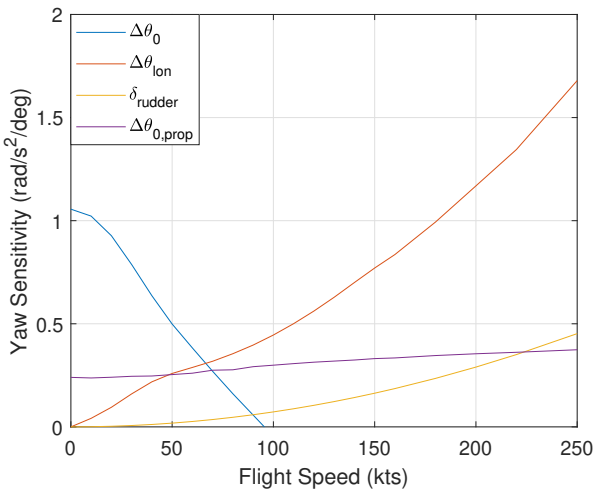

Figure 6. Yaw Sensitivities of Primary Yaw Controls

rotor disks toward or away from the flow (for forward flight conditions). This increases the upwash on one rotor and the downwash on the other, leading to a torque imbalance. The net flow into the rotors increases with flight speed, leading to the sensitivity increase observed in Fig. 6.

Propeller differential collective has a relatively constant yaw sensitivity over the flight envelope, which is lower in a unit sense ($\Delta\dot{r}_b/deg$) relative to differential collective ($\Delta\theta_0$) and differential longitudinal ($\Delta\theta_{lon}$) at their respective maximums. However, The propeller feathering range ($\pm$45 degrees) is much greater than the rudder or main rotor control range ($\pm$20 degrees), meaning the yaw control power of the propeller differential collective is still significant compared to the other available controls.

Differential collective on the main rotor is not used for yaw control above 60 kts due to the loss in yaw effectiveness (seen in Fig. 6) and roll coupling, shown in Fig. 7.

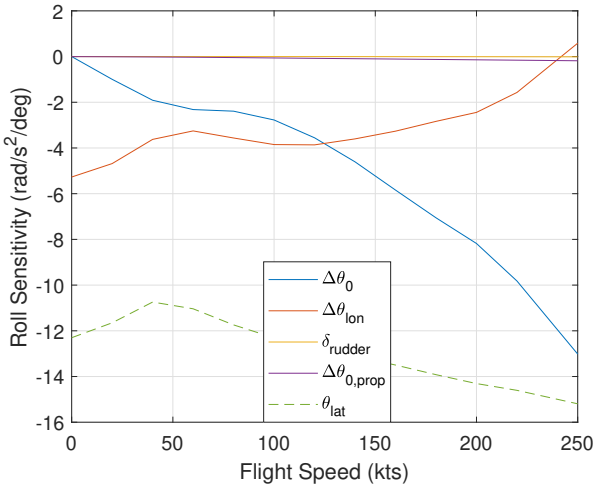

Figure 7. Roll Sensitivity of Yaw Controls

Summarizing Fig. 7, the rudder (δ_{rudder}) has no roll sensitivity due to zero vertical offset from the CG, and only functions as a yaw control. The differential longitudinal cyclic ($\Delta\theta_{lon}$) has a relatively small (compared to symmetric lateral cyclic, θ_{lat}) roll control sensitivity due to control phasing - scheduling the control phase angle with flight speed can improve this trend as well. Propeller differential collective ($\Delta\theta_{0,prop}$) has a low roll sensitivity which results from the use of counter-rotating propellers.

Most significantly, the differential collective ($\Delta\theta_0$) has a roll sensitivity that increases greatly with flight speed, due to the lack of roll moment balance on an individual rotor. One of the primary benefits of a coaxial rotor system is the possibility for lift offset, where the advancing side of a rotor is more heavily loaded than the retreating side, resulting in higher efficiency for the rotor system. However, if a differential collective input is applied to a coaxial rotor system with a non-zero lift offset, one rotor will increase the blade pitch on its advancing side, while the opposite rotor reduces its advancing side blade pitch. This results in a substantial roll moment imbalance, reflected in the roll control sensitivity. This control sensitivity increases with flight speed, in a similar shape as the lift offset target, to a level that's comparable to the control sensitivity of the intended roll control, symmetric lateral cyclic (θ_{lat}).

To get a full understanding of the yaw capability of the propellers compared to the other yaw controls, the control range must be taken into account. The available control range for the yaw controls is calculated by taking the maximum control limit and subtracting out the control value required for trimming the aircraft. For the one-sided control ranges, stall is ignored and only the geometric range is considered. The control range is multiplied by the (linearized) yaw control sensitivity to obtain the maximum yaw acceleration that can be produced by the yaw control mechanism. In short, the maximum yaw moment for each control is determined in a linear sense.

To determine whether or not each yaw control can provide *enough* yaw authority, the yaw control accelerations are compared to the requirements from ADS-33E PRF (Ref. 24), which gives values for yaw rate capability and the bandwidth for different levels of agility. A Level 1 aggressive yaw response represents the greatest agility. This requires in hover / low speed that the aircraft must be able to reach a yaw rate of 60 degrees per second and must have a yaw bandwidth of 3.5 rad/s. The yaw rate response is assumed as first order, a generic first order response with a time delay is shown in Eq. 10:

$$C(s) = \frac{K_r e^{-\tau_r s}}{T_r s + 1} \tag{10}$$

Where $C(s)$ is the response in the Laplace domain, K_r is the gain, τ_r is the time delay, and T_r is the time constant. The time constant T_r comes from the inverse of the bandwidth and the gain K_r is equal to the commanded yaw rate. Eq. 10 can be brought into the time domain in the form of Eq. 11:

$$c(t) = K_r(1 - e^{-\frac{t-\tau_r}{T_r}}) \tag{11}$$

Plugging in the desired values for the yaw rate and the yaw bandwidth results in the step response shown in Fig. 8. The maximum required acceleration of the aircraft can be determined from the time response by finding the maximum derivative. This occurs at the start of the step response following the time delay, with value given by Eq. 12:

$$\dot{c}_{max} = \dot{c}(\tau_r) = K_r(\frac{1}{T_r}) \tag{12}$$

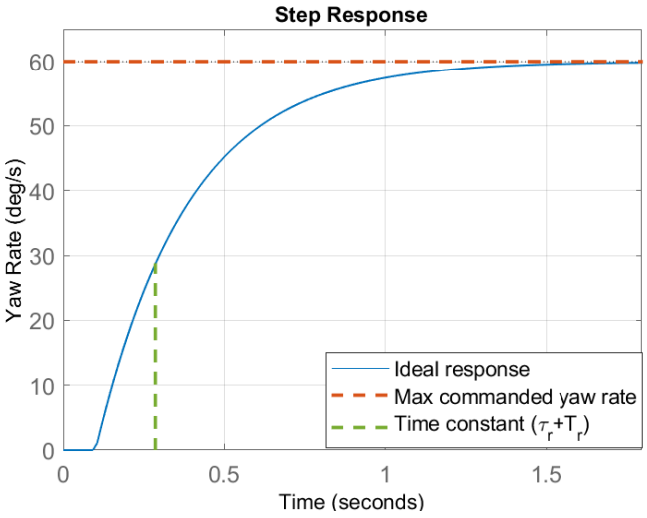

Figure 8. Ideal Yaw Step Response

Where $\dot{c}_{max}$ is the maximum acceleration, $\dot{c}(\tau_r)$ is the acceleration at the end of the time delay. This comes out to a maximum required acceleration of 60 deg/s $\times$ 3.5 rad/s $=$ 210 deg/s^2. This is plotted against the maximum yaw acceleration each control can generate in Fig. 9.

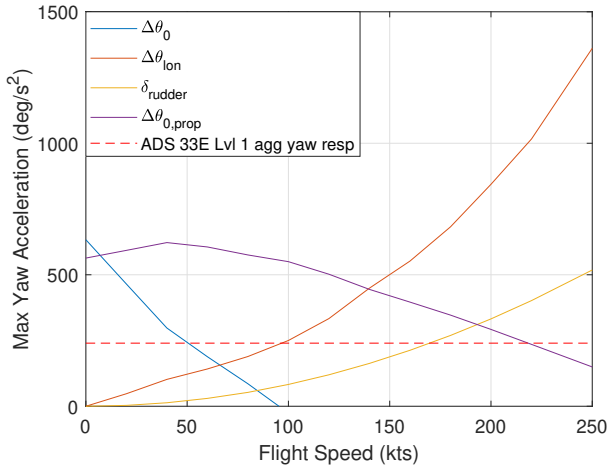

Figure 9. Maximum Yaw Acceleration

Differential collective ($\Delta\theta_0$), differential longitudinal ($\Delta\theta_{lon}$), and the rudder (δ_{rudder}) all follow similar trends to sensitivities. Considering these typical coaxial yaw control mechanisms, there is still a drop in yaw authority (below the dashed red line) around 50 to 100 kts. This implies that the maximum acceleration that can be generated by the differential collective, differential longitudinal, and the rudder deflection (by itself) is not great enough to meet the aggressive acceleration requirements from ADS-33E between 50 to 100 kts.

In this range, the differential propeller collective ($\Delta\theta_{0,prop}$) can generate a large maximum yaw acceleration compared to the other controls, due to the available control range of the propellers at low to mid speed. At these lower speeds, the required collective input for propulsive force balance is small and leaves a lot of room to feather the propellers for yaw control. As the flight speed increases, the required collective pitch on the propellers also increases leading to a smaller available range for differential inputs. Figure 9 shows that the range reduction causes the differential propeller maximum acceleration to fall off. Where the normal coaxial yaw controls fall below the yaw requirements, the dual propeller differential collective can provide the necessary acceleration.

HIGH SPEED

At high speed, an analysis is done to compare the capability of the dual propellers to the rudder. The aircraft uses the rudder alone at high speed for yaw control, therefore any failure of the rudder will lead to a loss of control if no action is taken. Previous work (Ref. 12) has shown that rudder failure in high speed flight (hard-out failure) is not something that the available main rotor controls can compensate for while maintaining sufficient rotor tip clearance. The dual propellers provide a redundant yaw control mechanism that can alleviate this issue. A trim case is performed where the rudder is set within a range of $\pm$20 degrees and the differential propeller setting is trimmed to counteract it. The results are displayed in Fig. 10.

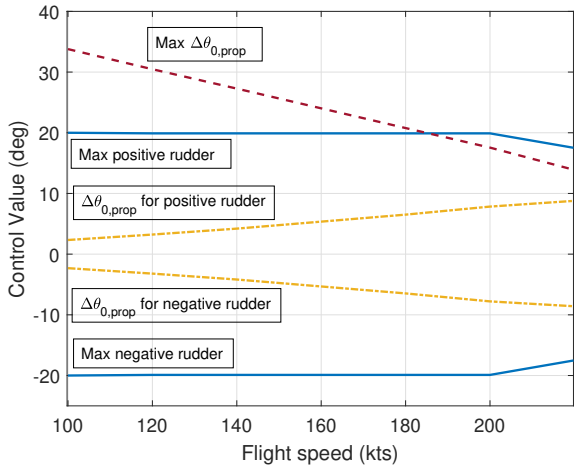

Figure 10. Trimmable Rudder Failure Range

Figure 10 shows the maximum trimmable rudder setting, the differential propeller setting required at that rudder position, and the available range of differential propeller (function of flight speed & ganged propeller collective). The available differential propeller range is calculated by subtracting the required collective propeller setting from the maximum one-sided propeller feathering range of 45 degrees. The solid lines indicate that the rudder can be set to its maximum positive and negative deflection at all speeds below 200 kts and trim can still be achieved with the differential propeller collective. The differential propeller setting required to handle this deflection is observed to be small compared to the maximum feathering range of the propeller.

The maximum trimmable rudder setting is ± 17.5 degrees above 200 kts, indicating that the aircraft cannot be trimmed in these speeds with the rudder at full deflection. The rudder is more effective at the higher flight speeds, resulting in a greater yaw moment being generated. However, propeller stall prevents the production of a large enough yaw moment to counter the rudder deflection. There is still available *geometric* range for the differential propeller setting to be increased, as indicated by comparing the dashed red line to the dashed yellow line, but aerodynamically there is not enough control margin available to allow for the full range of rudder deflection. In these extreme cases, rudder failure could be handled by either reducing the aircraft speed or allowing for some sideslip in normal operation.

CONCLUSIONS

This study investigates the effectiveness of dual side-mounted propellers as an additional form of yaw control. The helicopter (based on the X2 Technology™ Demonstrator) is modified to have two laterally mounted, counter-rotating propellers, and the aircraft is run through a series of test cases at low, moderate, and high speed flight. The following outcomes are observed:

1. At low speed, the trimmable outer ranges of the actuators (upper rotor upper limits, lower rotor lower limits) can be increased by using a differential collective input, balancing the net torque with the propellers until the propeller blade stalls. Inner actuator limits are set by tip clearance.

2. If the propeller stall limit is removed, upper rotor actuator maximum trim limit is increased past the geometric limit on the actuators. The lower rotor actuator minimums are limited by upper rotor stall.

3. Use of differential collective pitch of the propellers adds redundancy in the yaw control channel, the sensitivity of which is effectively constant over the flight envelope.

4. Differential propeller collective is able to compensate for the reduction in yaw control authority observed in the 50-100 kt range, increasing the yaw control power to allow for a Level 1 aggressive yaw response as prescribed by ADS-33E.

5. At high speed, the propellers function as a secondary yaw control capable of countering rudder failure. The aircraft can be trimmed with a full rudder deflection up to 200 kts, past which the tolerable rudder control range drops with the available differential collective pitch for the propellers, which is limited by blade stall.

AUTHOR CONTACT

Author	Contact
Alexander Stillman	stilla@rpi.edu
Michael McKay	michael.mckay005@gmail.com
Farhan Gandhi	fgandhi@rpi.edu

REFERENCES

1. F. Colucci, "FVL: Protected Across Domains," *Vertiflite*, no. 2, pp. 26–29, 2022.

2. G. Jacobellis, F. Gandhi, and M. Floros, "Using Control Redundancy for Power and Vibration Reduction on a Coaxial Rotor Helicopter at High Speeds," *Journal of the American Helicopter Society*, vol. 64, pp. 1–15, July 2019.

3. T. Herrmann, R. Celi, and J. Baeder, "Multidisciplinary Trim Analysis of a Coaxial-Pusher Rotorcraft Configuration," in *American Helicopter Society 74th Annual Forum, Phoenix, AZ*, May 2018.

4. T. Herrmann, R. Celi, and J. Baeder, "Multidisciplinary, Multiobjective Trim Optimization for a Coaxial-Pusher Rotorcraft Configuration," in *Vertical Flight Society 75th Annual Forum, Philadelphia, PA*, May 2019.

5. G. Jacobellis, P. Anusonti-Inthra, and F. Gandhi, "Investigation of Blade Loads on a Modern High-Speed Lift-Offset Coaxial Helicopter using Coupled Computational Fluid Dynamics / Computational Structural Dynamics," in *AHS Aeromechanics Specialists' Meeting, San Francisco, CA*, Jan. 2018.

6. P. Singh, *Aeromechanics of Coaxial Helicopters using the Viscous Vortex Particle Method*. PhD Thesis, University of Michigan, 2020.

7. T. Berger, O. Juhasz, M. J. Lopez, and M. B. Tischler, "Modeling and Control of Lift Offset Coaxial and Tiltrotor Aircraft," in *44th European Rotorcraft Forum, Delft, The Netherlands*, Sept. 2018.

8. T. Berger, O. Juhasz, M. J. S. Lopez, M. B. Tischler, and J. F. Horn, "Modeling and Control of Lift Offset Coaxial and Tiltrotor Rotorcraft," *CEAS Aeronautical Journal*, 2019.

9. T. Berger, C. L. Blanken, M. B. Tischler, and J. F. Horn, "Flight Control Design and Simulation Handling Qualities Assessment of High-Speed Rotorcraft," in *Vertical Flight Society 75th Annual Forum, Philadelphia, PA*, May 2019.

10. T. Berger, M. B. Tischler, and J. F. Horn, "Outer-Loop Control Design and Simulation Handling Qualities Assessment for a Coaxial-Compound Helicopter and Tiltrotor," in *Vertical Flight Society 76th Annual Forum, Virtual*, Oct. 2020.

11. M. McKay, P. Vayalali, and F. Gandhi, "Post-Failure Control Reconfiguration on a High-Speed Lift-Offset Coaxial Helicopter," in *American Helicopter Society 76th Annual Forum (Virtual)*, Oct. 2020.

12. M. McKay, P. Vayalali, and F. Gandhi, "Redistributed Allocation for Flight Control Failure on a Coaxial Helicopter," in *American Helicopter Society 77th Annual Forum (Virtual)*, May 2021.

13. M. E. McKay, *Fault Tolerant Control of Multirotor Vehicles*. PhD Thesis, Rensselaer Polytechnic Institute, 2021.

14. F. Frey, J. Thiemerier, C. Ohrle, M. Kebler, and E. Kramer, "Aerodynamic Interactions on Airbus Helicopters' Compound Helicopter RACER in Cruise Flight," *Journal of the American Helicopter Society*, vol. 65, pp. 1–14(14), Oct. 2020.

15. R. Huot and P. Eglin, "Flight Mechanics of the RACER Compound H/C," in *Vertical Flight Society 76th Annual Forum, Virtual*, Oct. 2020.

16. Airbus, "X3 Celebrating a game-changing high-speed demonstrator," in *https://www.airbus.com/en/who-we-are/our-history/helicopters-history/x3, Accessed 04-03-2022*.

17. A. Ruddell, "Advancing Blade Concept (ABC) Technology Demonstrator," TR 81-D-5, AVRADCOM, Apr. 1981.

18. J. P. Reddinger and F. Gandhi, "Using Redundant Effectors to Trim a Compound Helicopter with Damaged Main Rotor Controls," in *American Helicopter Society 73rd Annual Forum, Fort Worth, TX*, May 2017.

19. Y. B. Kong, J. V. R. Prasad, and D. Peters, "Development of a Finite State Dynamic Inflow Model for Coaxial Rotor using Analytical Methods," in *American Helicopter Society 73rd Annual Forum, Fort Worth, TX*, May 2017.

20. R. D. Harrington, "Full-Scale-Tunnel Investigation of the Static-Thrust Performance of a Coaxial Helicopter Rotor," techreport 2318, National Advisory Commitee For Aeronautics (NACA), Mar. 1951.

21. R. Feil, J. Rauleder, C. Cameron, and J. Sirohi, "Aeromechanics Analysis of a High Advance Ratio Lift Offset Coaxial Rotor System," *Journal of Aircraft*, vol. 56, pp. 166–178, Jan. 2019.

22. S. W. Ferguson, "A Mathematical Model for Real Time Flight Simulation of a Generic Tilt-Rotor Aircraft," CR 166536, NASA, Sept. 1988.

23. B. W. McCormick, *Aerodynamics, Aeronautics, and Flight Mechanics*. New York, NY: John Wiley & Sons, 1995.

24. Anon, "Handling Qualities Requirements for Military Rotorcraft," tech. rep., Aeronautical Design Standard and Performance, Specification ADS-33E-PRF, US Army Aviation and Missile Command, 2000.